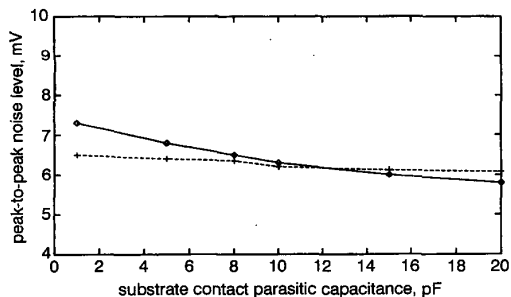


**Experimental setup:** To evaluate the effectiveness of the active substrate coupling noise reduction method, several test chips have been fabricated through the MOSIS 1.2 $\mu$ m NMOS process. A circuit framework for SPICE simulation was also set up for the negative feedback noise reduction technique. The testing and simulation results will be presented in the results Section. This test chip has 40 pins with an area of 1941  $\times$  1935 $\mu$ m<sup>2</sup>. Three digital circuit blocks were built on the chip. Each block was made of a chain of inverters. This setup is used to simulate the random switching scenario of a typical digital circuit. A switching signal can be injected into the chip from the input stage of each inverter chain. It can accommodate three different switching frequencies running inside the chip. Six analogue NMOS transistors are arranged as a 2  $\times$  3 array to measure the noise at different locations.

Substrate contacts were placed on both the analogue side and the digital side of the chip. A reference line dividing the analogue portion and digital portion of the chip was laid in the middle of the contacts (Fig. 2). The substrate contact on the analogue portion of the chip, called the sample contact, had a fixed distance of 50 $\mu$ m from the reference line. A substrate contact on the digital portion of the chip, called the re-inject contact, was placed on the mirrored side of the sample contact. An on-chip two stage op-amp is embedded to form the negative feedback loop. The positive input of the amplifier is connected to ground while the negative input is connected to a different sample contact. The output of the op-amp is connected to the re-inject contact. This arrangement creates a virtual ground for the negative input of the amplifier which has the same potential as that of the substrate.

**Results:** Fig. 3 shows the noise reduction against frequency of the digital noise. The gain-bandwidth product of the on-chip amplifier is 7.6MHz. The experiment and simulation show that on average, the active noise reduction method can decrease the measured noise level to 17% of its original value if the digital operating frequency is less than 1MHz. The noise increases after the digital operating frequency passes 1MHz. Fig. 4 shows the rescaled plots containing only the reduced noise value with an operating frequency of <1.2MHz. The plots show that the measured noise level was higher (38% higher) than the simulated value. This can be explained by the noise coupled into the probe during testing. This demonstrated that the noise frequency has a profound impact on the noise reduction outcome due to the limitation of the gain-bandwidth product.



**Fig. 5 Peak-to-peak noise against contact area**  
Parasitic capacitance has linear relation with contact area  
◇ sample contact  
+ re-inject contact

One important decision is the geometric size (area) of the substrate contacts. Fig. 5 shows the relationship between contact area (parasitic capacitance) and the noise level. Since only the area of the contact, which determines the value of capacitor  $C_1$  and  $C_2$  in the circuit model, has an influence on the capacitance. The geometric shape can be arbitrary. We can conclude that the area of the re-inject contact has a larger effect on the reduced noise level than the sample contact.

**Conclusion:** The active noise reduction method achieved 83% noise reduction with a proper negative feedback loop installed. Because

this technique works well for mixed-signal designs operating at lower frequencies, it will be most useful in low power portable electronics with slower digital clock speeds. This active method also has the merit that it is independent of the traditional noise reduction methods and thus can be used in combination with them (e.g. guard rings). Further testing is being conducted with more complex test chips.

© IEE 1999  
Electronics Letters Online No: 19991127  
DOI: 10.1049/el:19991127

5 August 1999

Tingyang Liu, J.D. Carothers and W.T. Holman (Department of Electrical and Computer Engineering, The University of Arizona, Tucson, AZ 85721, USA)

E-mail: carothers@ece.arizona.edu

## References

- 1 SU, D.K., LOINAZ, M.J., MASUI, S., and WOOLEY, B.A.: 'Experimental results and modeling techniques for substrate noise in mixed-signal integrated circuits', *IEEE J. Solid-State Circuits*, 1993, **28**, (4), pp. 420-430
- 2 ARAGONES, X., MOLL, F., ROCA, M., and RUBJO, A.: 'Analysis and modelling of parasitic substrate coupling in CMOS circuits', *IEE Proc. Circuits Devices Syst.*, 1995, **142**, (5), pp. 307-312
- 3 BLALACK, T., LAU, J., CLEMENT, F.J.R., and WOOLEY, B.A.: 'Experimental results and modeling of noise coupling in a lightly doped substrate'. IEEE 1996 Int. Electron Devices Meeting, 1996, pp. 23.3.1-23.3.4
- 4 FORBES, L., FICQ, B., and SAVAGE, S.: 'Resonant forward-biased guard-ring diodes for suppression of substrate noise in mixed-mode CMOS circuits', *Electron. Lett.*, 1995, **31**, (9), pp. 720-721
- 5 MAKIE-FUKUDA, K., MAEDA, S., TSUKADA, T., and MATSUURA, T.: 'Substrate noise reduction using active guard band filter in mixed-signal integrated circuits', *IEICE Trans. Fundamentals*, 1997, **E80-A**, (2), pp. 313-320

## RF circulator structures via offset lithography

P.S.A. Evans, P.M. Harrey, B.J. Ramsey and D.J. Harrison

Further developments are reported of the conductive lithographic film (CLF) process in which components of radio-frequency circulators are fabricated economically via offset lithography. The performance of centre conductor elements printed from silver-loaded inks on polymer substrates is compared with that of conventional solid copper structures.

The conductive lithographic film (CLF) process employs standard offset lithographic printing technology to fabricate conductive patterns on a wide range of flexible substrates using purpose-developed conductive inks. These inks consist primarily of electrically conductive (silver) particles having a mean particle size of  $\sim$ 1 $\mu$ m suspended in an organic resin, and are compatible with a wide range of organic and synthetic substrates. When printed and air-dried, the inks yield electrical conductors with a sheet resistivity of  $\sim$ 0.15 $\Omega/\square$ .

The ink films are robust, withstanding a range of standard environmental test regimes applied to conventional etched copper laminate wiring boards. CLF substrates also exhibit excellent dimensional control and registration, and track-and-gap spacings of 100 $\mu$ m are readily achieved. The principal advantage of the process is that CLF substrates can be manufactured very rapidly via a one-stage printing operation and are consequently cheap to produce. Typical manufacturing costs are  $\sim$ 1% of those incurred in etching solid copper circulator conductors from sheet metal.

**Microwave circulators:** Microwave circulators operating above 100MHz are employed as non-reciprocal elements to combine transmitter and receiver systems with common antennas while protecting the receivers from the transmitter output power. The devices are employed in telecommunications, radar and related

systems. However, the high cost of conventional circulators has restricted their use to essential or cost-insensitive applications.

Conventional coaxial circulators are constructed by creating a cavity in the coaxial line, and modifying the centre conductor to form a circular-form structure with port terminations arranged around its periphery. The conductor dimensions largely govern the operating frequency of the device. On each side of the conductor are mounted precision-ground sections of ferrite. The entire assembly is polarised by an external static magnetic field acting normal to the plane of the conductor.

Recent work has established the viability of microwave stripline structures, coplanar waveguides, ring resonators, couplers and antennas printed onto various flexible substrate materials by the CLF process [1, 2].

More recently, passive components and low-frequency filter systems have been entirely fabricated via offset lithography [3, 4]. In this Letter we report the evaluation of silver ink films printed on polyethylene substrates as substitutes for silver-plated copper conductors in UHF circulator assemblies. The purpose of this work was to establish the functionality of CLF films as circulator conductor elements, and evaluate the metal losses and impedance matching of these films in comparison with conventional silver-plated copper components.

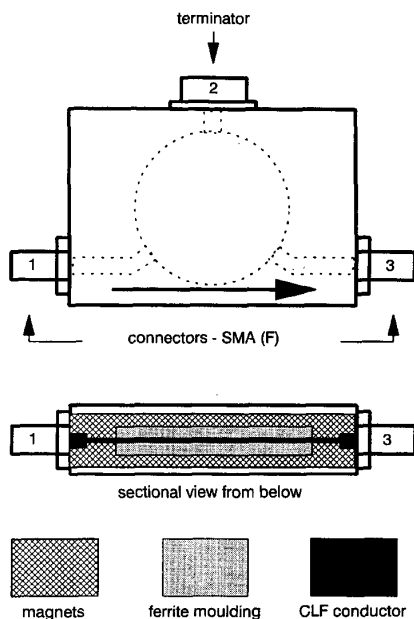


Fig. 1 Circulator cavity housing

**Printed circulator conductor design:** A circulator conductor design developed by RT Microwave was prepared on a standard lithographic printing plate. Conductive patterns were printed on 230 $\mu$ m thick 'Polyart', a polyethylene film paper substitute found to possess well controlled dielectric properties. Both sides of the substrate were printed, with the ink film patterns registered to within 0.05mm.

To evaluate the effect of metal losses arising from the sheet resistivity of CLF conductors on the circulator performance, a proportion of the printed substrates were electroplated using a proprietary silver plating process. 2 $\mu$ m of plated silver were deposited on these films, reducing the sheet resistivity to  $\leq 0.05\Omega/\square$ .

Circulator assemblies were constructed containing CLF, silver-plated CLF and silver-plated copper conductors. Each assembly comprised one type of centre conductor, mounted in a conventional circulator cavity assembly (Fig. 1) containing bulk ferrite mouldings and polarising magnets which applied a field normal to the plane of the CLF conductor. Contact between the assembly SMA connectors and printed ink films was achieved by a silver-loaded adhesive.

The circulators were evaluated using a standard test installation comprising a Wiltron 5409A network analyser, a VSWR measure-

ment head (Wiltron 'autotester' type 5400-6N50) and an RF detector (Wiltron 5400-71N50). The second port of each circulator was terminated by a 50 $\Omega$  resistive terminator (Florida Labs. type 42-1008).

The test apparatus evaluated each of the circulator metallisations, measurements being made of the transmission loss (port 1 – port 3), reverse-loss and return-loss (port 3 – port 1) of the circulators at 3 MHz intervals in the frequency range 440–460MHz.

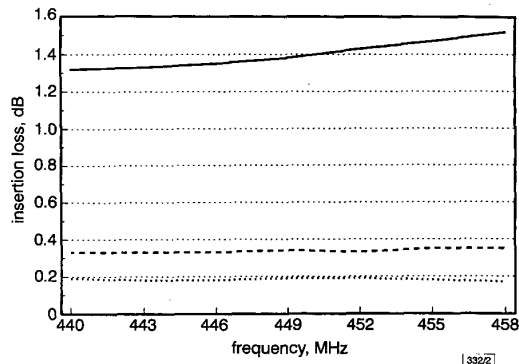


Fig. 2 Circulator insertion losses

— CLF conductor  
 --- silver-plated CLF conductor  
 ..... copper conductor

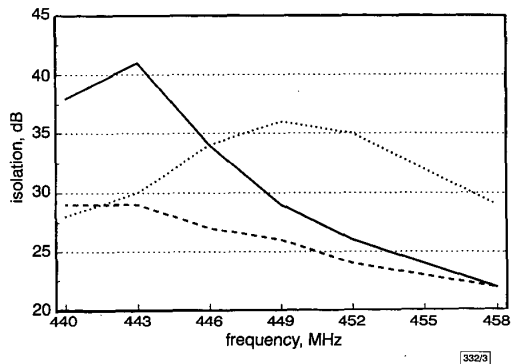


Fig. 3 Circulator isolation losses

— CLF conductor  
 --- silver-plated CLF conductor  
 ..... copper conductor

These results are summarised in Figs. 2 and 3. Referring to these Figures, it can be seen that the CLF centre conductor yielded an isolation (reverse-loss) of 41 dB at 443MHz with a corresponding transmission loss of 1.3dB. This relatively high isolation figure is considered to be influenced by the finite metal losses of the CLF conductors which further attenuate signals reflected at port 3.

Circulator assemblies containing CLF conductors plated with 2 $\mu$ m of metallic silver exhibited isolation and transmission losses more closely approximating the conventional etched-copper centre conductors. A maximum isolation of 36dB occurred at 449MHz with a corresponding transmission loss of 0.35dB. The finite resistivity of the silver-plated CLF conductor, although significantly reduced by the plating process, is again considered to increase the measured isolation.

The solid copper conductor employed as a reference exhibited maximal isolation at 443MHz, with a corresponding transmission loss of 0.2dB.

**Conclusions:** Microwave circulator centre conductors printed on polymer substrates have been evaluated in comparison with conventional plated copper structures. The results indicate that acceptable circulator performance is readily achieved with both plated and non-plated printed conductors produced by the CLF process. These substrates were produced at high speed, and at

greatly reduced cost compared to the conventional silver-plated copper conductor employed as a reference.

Unplated CLF conductors exhibited through losses of 1.3dB at 443MHz, which may be acceptable in low cost applications. Silver plated CLF film conductors are found to exhibit losses similar to those of solid copper structures while retaining many of the advantages of the CLF process. It is therefore considered that CLF substrates offer a rapid and cost effective means of manufacturing RF circulator conductors. Future work will entail the fabrication of other circulator components by the offset lithographic printing process.

**Acknowledgments:** The authors thank R.F. Sims and M.C. Sweetland of R.T. Microwave Ltd. (Barton-Under-Needwood), J. Cooper of Arjobox Synthetic Papers Ltd (Clacton-On-Sea), and P.R. Shepherd of the University of Bath for their collaboration in aspects this work, which was partially funded under EPSRC grant No. GR/L8612.

© IEE 1999

Electronics Letters Online No: 19991131  
DOI: 10.1049/el:19991131

15 July 1999

P.S.A. Evans, P.M. Harrey, B.J. Ramsey and D.J. Harrison  
(Department of Design, Brunel University, Uxbridge, Surrey, TW20 0JZ, United Kingdom)

## References

- EVANS, P.S.A., RAMSEY, B.J., HARRISON, D.J., and SHEPHERD, P.R.: 'Assessment of conductive lithographic films for microwave applications'. Automated RF and Microwave Measurement Society Conf., Limpley Stoke, Bath, UK, 31 Oct. - 15 Nov. 1996
- EVANS, P.S.A., RAMSEY, B.J., HARRISON, D.J., and SHEPHERD, P.R.: 'Lithographic technology for microwave integrated circuits', *Electron. Lett.*, 1997, **33**, (6), pp. 483-484
- HARREY, P.M., EVANS, P.S.A., RAMSEY, B.J., and HARRISON, D.J.: 'A novel manufacturing process for capacitors using offset lithography'. 1st Int. Symp. Environmentally Conscious Design and Inverse Manufacturing, Tokyo, Japan, 1-3 Feb. 1999
- EVANS, P.S.A., RAMSEY, B.J., HARREY, P.M., and HARRISON, D.J.: 'Printed analogue filter structures', *Electron. Lett.*, 1999, **35**, (4), pp. 306-308

## Record-high reflectance in narrowband low-loss Bragg reflectors with Si-on-LiNbO<sub>3</sub> waveguides

H. Feng, R.F. Tavlykaev and R.V. Ramaswamy

A 6.5mm long waveguide reflector with 88% reflectance and 4.3Å bandwidth at 1.5µm has been realised using an LiNbO<sub>3</sub> waveguide with an Si overlay. The thickness of the latter was chosen so as to yield both high reflectance and low propagation loss, in conformance with the previously developed theoretical model.

**Introduction:** The development of high-reflectance waveguide gratings in ferroelectrics, such as LiNbO<sub>3</sub> and the like, has long been hindered by a number of inherent difficulties. On the other hand, such gratings are needed, for example, for waveguide laser applications [1]. Recently, LiNbO<sub>3</sub> waveguides with Si overlays have been proposed for use in high-reflectance low-loss gratings, even though their intriguing modal behaviour was not fully understood at the time [2]. Subsequently, the modal behaviour has been analysed theoretically [3]. The developed theoretical model underscored the unusual properties of the composite waveguide structure and confirmed the unique possibility of achieving a large perturbation of the effective mode index and low loss at the same time, which are the necessary conditions for achieving low-loss high-reflectance gratings. Furthermore, the theory predicted a periodic dependence of loss and index perturbation against the thickness of the Si overlay.

In this Letter we report the results of an experimental study performed to verify theory and maximise the reflectance of DBRs

formed in LiNbO<sub>3</sub> waveguides with Si overlays. By choosing the correct Si thickness, we have realised a waveguide DBR with 88% reflectance and 4.3Å bandwidth at a centre wavelength of 1513 nm. The achieved reflectance is, to the best of our knowledge, the highest for waveguide gratings in LiNbO<sub>3</sub> waveguides reported thus far.

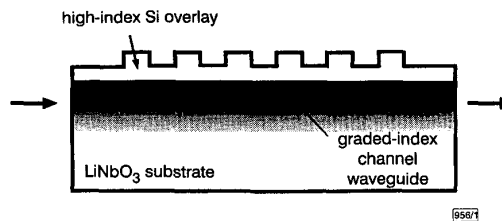


Fig. 1 Longitudinal cross-section of DBR comprising LiNbO<sub>3</sub> waveguide and high-index Si overlay

**Outline of theoretical analysis:** The key feature of the corrugated Si-on-LiNbO<sub>3</sub> DBR in Fig. 1 is the use of an Si overlay to substantially perturb the mode index of the underlying optical waveguide in LiNbO<sub>3</sub>. Si is the material of choice due to its processibility, low cost, and most importantly its large refractive index (~3.4 at 1.5µm) which enables a large index perturbation to be obtained. The high refractive index of the Si overlay strongly affects the effective mode index of the entire composite structure. In particular, the mode index is modified if the Si thickness changes. Hence, modulation of the mode index can be obtained by forming a corrugated Si overlay as illustrated in Fig. 1. A surprising behaviour was observed [2] in that even thick Si films, capable of supporting multiple planar modes by themselves did not necessarily have a measurable effect on the loss and the field distribution of the underlying LiNbO<sub>3</sub> singlemode channel waveguide, while the effective mode index was significantly affected.

Recently, we have shown that this unusual behaviour results from rapid mode evolution with increasing Si thickness when the power carried by a guided mode is redistributed between Si and LiNbO<sub>3</sub>. The field of a guided mode of the composite Si-on-LiNbO<sub>3</sub> structure near cut-off resides in LiNbO<sub>3</sub>, rather than in Si. As a result, all guided modes, except for the highest-order mode, are tightly confined in the Si overlay and suffer loss as they propagate along the structure. In contrast, the highest-order mode has most of its field localised in LiNbO<sub>3</sub>. As such, the effect of intrinsic loss of Si on the propagation loss of the highest-order mode is dramatically diminished and the latter propagates with low loss. At the output, this mode may resemble the fundamental mode of the LiNbO<sub>3</sub> waveguide, however, with a significantly modified (increased) mode index.

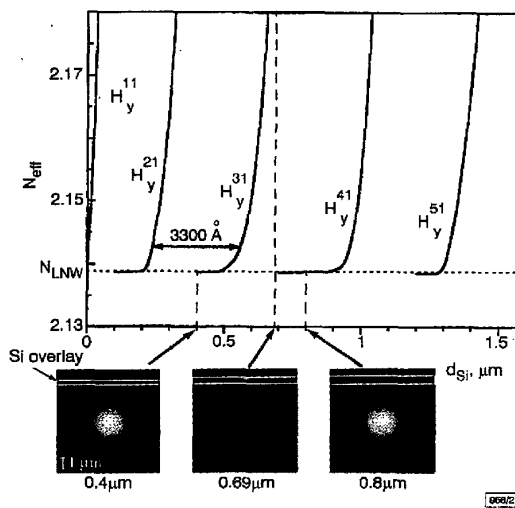


Fig. 2 Effective mode index of Si-on-LiNbO<sub>3</sub> structure against Si thickness

See [3] for details; intensity plots show transverse distribution of highest-order mode for Si thickness of 0.4µm (cutoff for H<sub>y</sub><sup>31</sup> mode), 0.69µm (H<sub>y</sub><sup>31</sup> mode confined in Si overlay), and 0.8µm (cutoff for H<sub>y</sub><sup>41</sup> mode)